Physica D 48 (1991) 1–16
North-Holland

PERIODIC TO QUASIPERIODIC TRANSITION OF CHEMICAL SPIRAL ROTATION

Gordon S. SKINNER and Harry L. SWINNEY
Center for Nonlinear Dynamics and the Department of Physics, The University of Texas at Austin, Austin, TX 78712 USA

Received 2 March 1990
Revised manuscript received 9 September 1990
Accepted 9 September 1990
Communicated by A.T. Winfree

We report observations of the tip motion of spiral waves in excitable Belousov–Zhabotinskii reagent. An open reactor is used to determine the *time-asymptotic* dynamics of the spiral tip as a function of a control parameter. We have observed a supercritical transition from simple rotation (one frequency) to compound rotation (two frequencies); the compound motion at onset closely resembles that predicted by two-species reaction–diffusion models. Measurements of the frequencies of the motion indicate that the compound rotation is quasiperiodic over the range studied; there is no evidence of frequency locking. The compound tip motion appears to result from fluctuations in the curvature of the spiral wave near its tip. We describe qualitatively the sequence of events during a single tip orbit and suggest that the refractory tail of the wave plays a dominant role in controlling the tip motion.

1. Introduction

Rotating spiral waves have long elicited the attention of researchers in a host of different fields, including biology, cardiology, chemistry, and mathematics. Perhaps the most extensively studied medium in which spirals are manifest is the Belousov–Zhabotinskii (BZ) reagent – blue waves of oxidation propagating in a thin layer of reduced (red) reagent can be broken, with each break eventually developing into a pair of spirals [1] (plate Ia). The chemical basis of the medium makes the study of these spirals simpler than that of spirals in other physical excitable media such as heart muscle [2] or social amoeba colonies [3].

1.1. Motion of the spiral tip

Two questions naturally arise concerning spiral waves in excitable media. First, what is the shape of the spiral wave? Second, is it a stable shape (invariant under rotation and time translation), and if it is not stable, how is it changing in time? That is, what are the *dynamics* of the spiral?

The first question has been carefully addressed experimentally [4] and theoretically [5] for the BZ reagent. A unique, invariant shape has been found in some conditions in laboratory experiments and numerical simulations. In these instances, the *tip* of the spiral traces a circular path that encloses a central core region. For other conditions, however, the spiral does *not* assume a stable shape. The tip then follows a distinctly noncircular trajectory [6–10]. Such behavior has also been observed in cardiac tissue [2] and in simulations of various excitable media [9, 11–19].

The term *meander* was coined for the noncircular motion by Winfree [6] before it was studied under close scrutiny; boundary effects, hydrodynamics, and inhomogeneities all took part in producing a net motion that appeared quite irregular. Jahnke, Skaggs, and Winfree [9] later observed that in the BZ reagent spiral meander is not an artifact due to external influences, but is evidently inherent in the chemistry used. Their chemical and numerical experiments revealed circular tip orbits for some chemistries and epicycle-like orbits for others, as shown in fig. 1.

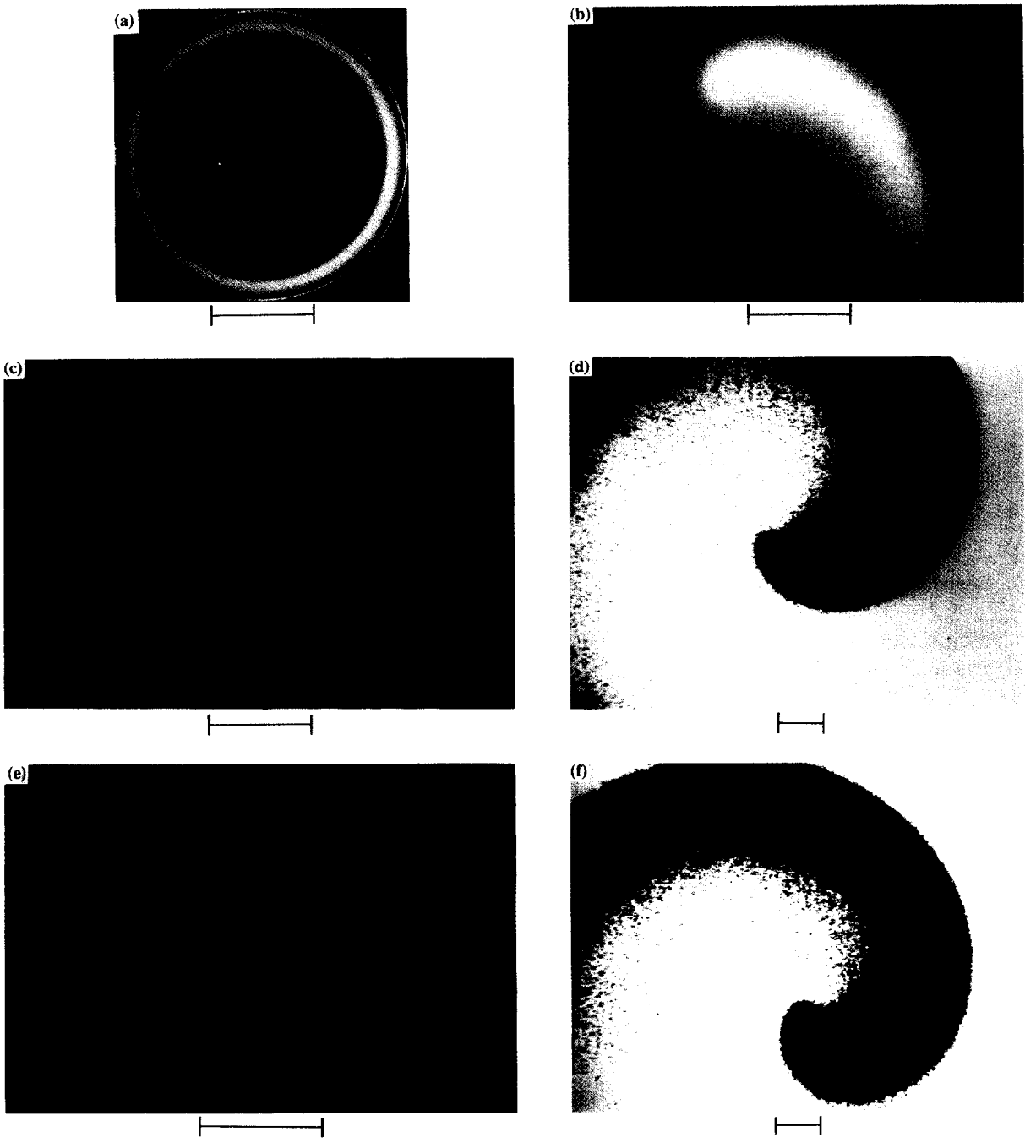
(a)
(b)
(c)
(d)
(e)
(f)

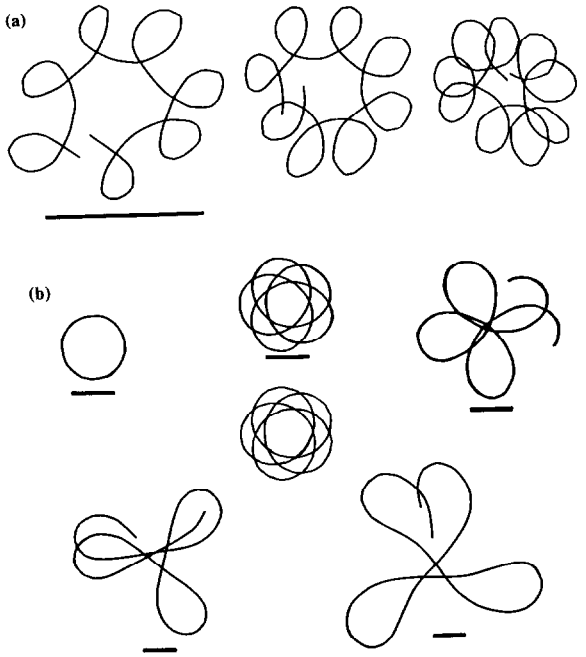

Fig. 1. (a) Experimental tip orbits for a single spiral in a petri dish, from Jahnke et al. [9]. The three orbits (traced chronologically from left to right) show the effect of the reagent aging. The bar represents 1 mm. (b) Computer-generated spiral tip orbits using a two-variable Oregonator model, for several different values of the parameter f ("coefficient of stoichiometry" in the model), also from ref. [9]: top row from left to right, $f = 1.6$, $f = 1.8$ (lower figure is an epicycle shown for comparison), $f = 2.0$; bottom row from left to right, $f = 3.0$, $f = 4.0$. The bars represent 0.18 mm.

Our experiments demonstrate that for a wide variety of chemistries, the noncircular tip motion observed in the absence of external effects is described by two frequencies – we refer to the motion as *compound rotation*.

1.2. The CFUR: an open-system for study of spirals

The petri dish experiments of Jahnke et al. (fig. 1a) illustrate a problem with past experiments: they were not controllable because they were performed on *closed* systems. The experiments were performed by initially establishing a nonequilibrium state and observing any spirals that formed as the medium decayed to equilibrium. Studies of stability or bifurcations were not possible because the only time-asymptotic state accessible in the experiments was thermodynamic equilibrium. In the study of temporal BZ reagent dynamics, a type of *open* system, the continuously stirred tank reactor (CSTR), is often employed to maintain the reaction at a fixed distance from equilibrium by establishing a net flux of reagent through the system. Of course, the CSTR is not suitable for studies of spatial patterns such as spiral waves because the stirring quickly destroys any patterns that emerge.

An open system suitable for the study of spatial chemical patterns is the continuously fed unstirred reactor (CFUR) recently developed by Tam et al. [20]. Like the CSTR, the CFUR maintains the reaction at a constant distance from equilibrium, but it differs in that the flow of reagent that maintains the nonequilibrium state is diffusive, not advective, so that spirals and other spatial patterns that evolve are governed solely by the interplay of reaction and diffusion. The patterns can be maintained indefinitely and measured quantitatively as a function of the external control parameters.

◂Plate I. (a) A pair of counterrotating spirals in the CFUR (described in the text), illuminated with a fluorescent ring lamp ($[KBrO_3] = 0.05$ M, all other concentrations are as given in section 2.1; the white border around the gel is a teflon spacer ring). (b) Video image of a spiral tip ($[KBrO_3] = 0.028$ M); this tip is the first one in (c) below. Compare (b) with the images in (c)–(f), which have been processed using false color. (c) Superposition of a single tip, showing simple rotation, at times separated by 2 min (this was a transient orbit near $[KBrO_3] = 0.028$ M). (d) Spiral tip exhibiting compound rotation with a maximum wave front curvature of 0.7 mm^{-1} ($[KBrO_3] = 0.040$ M). (e) Superposition of a single tip, showing compound rotation, at times separated by 1.5 min; the apparent "notch" in the second to last tip is due to a scratch in the reactor window ($[KBrO_3] = 0.040$ M). (f) Same tip as in (d), 3 min later; the maximum front curvature is 2.0 mm^{-1} (image rotated by 180° to aid comparison). (d) and (f) were processed using 32 intensity bands, 8 gray levels per band; the colors are uncorrelated with those in (c) and (e). The arrows in (c) and (e) merely indicate direction of rotation; they do not depict the tip trajectory defined by the experiment. The bar in (a) represents 10 mm; in (b) through (f), 1 mm.

We have used a CFUR to study the time-asymptotic dynamics of spiral tip motion in a two-dimensional disk of BZ reagent. A small region near the center of the spiral was monitored with a video camera, and image processing was performed to define the tip of the spiral and follow its path through the medium. We have determined from these observations that, as a control parameter (potassium bromate concentration) is increased, the motion of the tip undergoes a transition from simple, circular rotation, as shown in plate Ic, to compound rotation suggestive of epicycles, as shown in plate Ie. No hysteresis has been found – the transition appears to be supercritical. By measuring the intensity at a point as a function of time, we have determined the two frequencies that characterize the orbit, and we have measured the frequencies as a function of control parameter. Finally, we report some qualitative observations regarding the curvature of the spiral tip as it undergoes compound rotation.

2. Experimental techniques

Fig. 2 shows a scale cutaway view and plate Ia shows a top view of the CFUR used in our experiments [20]. The basic operation of the CFUR is as follows. The reactant solutions are pumped continuously into a vigorously stirred reservoir. The reservoir, a CSTR, couples to a thin, circular gel layer by *diffusive* transport through a glass capillary array and a filter membrane. The reagent in the gel attains an asymptotic, nonequilibrium state in which reaction–diffusion patterns can form. The patterns are illuminated and viewed through a quartz window that is in contact with the gel.

2.1. Chemical procedures

The reactants were delivered to the reservoir in four separate feeds, listed here with their reservoir concentrations: (1) malonic acid ($CH_2(COOH)_2$), 0.05 M, and ferroin ($Fe^{+2}(phen)_3$),

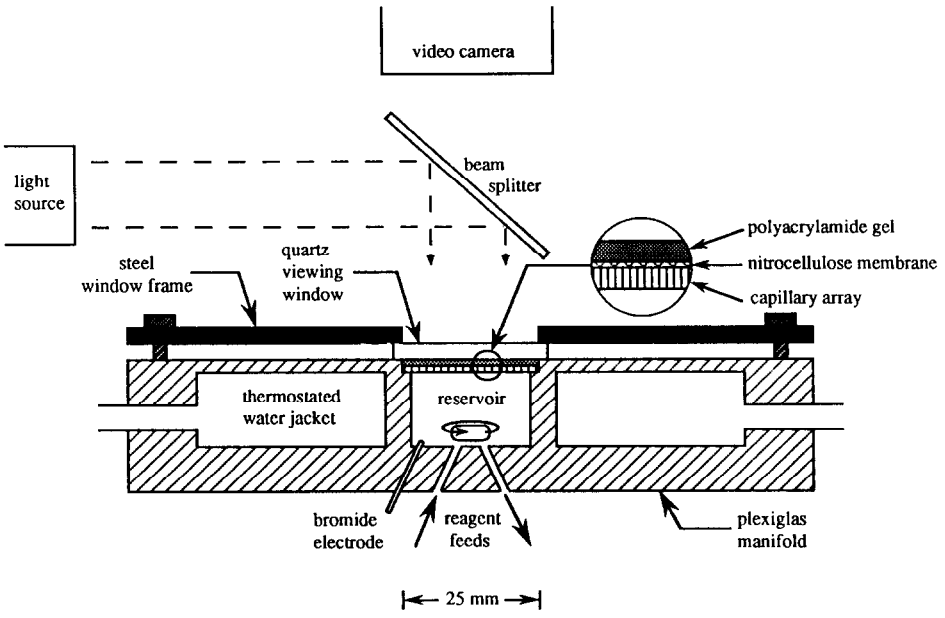

Fig. 2. Scale cutaway of the continuously fed unstirred reactor (CFUR). The reactor is cylindrically symmetric about its vertical midline. The inset shows a detailed cross section of the circular gel assembly.

0.0025 M, (2) sulfuric acid (H_2SO_4), 0.2 M, and potassium bromide (KBr), 1.0×10^{-4} M, (3) potassium bromate ($KBrO_3$), 0.2–1.0 M and (4) distilled water. The potassium bromate concentration was varied by adjusting the flow rate of its pump, while maintaining a constant total flow rate into the reservoir by compensating with the flow rate of the water pump. The flow rates for feeds (1) and (2) were each 10 ml/h. The flow rate for feeds (3) and (4) together was also 10 ml/h, making the total flow rate 30 ml/h in all experiments. This gave a CSTR residence time (volume/flow rate) of 10.6 min, given our reservoir volume of 5.3 ml.

All solutions were made using distilled deionized water, and molarities were determined by using the formula weights and specific gravities of the reagent grade stock chemicals. The potassium bromate was recrystallized twice from aqueous solutions. The malonic acid was recrystallized three times using ethyl acetate and acetone-chloroform as solvents, using the recipe of Noszticzius et al. [21]. The ferroin was made from $Fe(NH_4)_2(SO_4)_2$ and 1,10-phenanthroline in the stoichiometric 1:3 ratio, with a 4.4% excess of 1,10-phenanthroline to assure a minimal degree of dissociation. The potassium bromide was singly recrystallized from an aqueous solution.

It was important to have a nonoscillatory (excitable) chemical state in the reservoir because oscillations in the reservoir strongly perturbed the patterns in the gel, making them become faint and distorted. Potassium bromide was included in the reactants for the sole purpose of eliminating oscillations. According to the Field–Körös–Noyes (FKN) mechanism of the BZ reaction [22], an oscillation (red–blue–red) is initiated when the concentration of bromide ions drops below a critical level, allowing "process B" of the mechanism to dominate over "process A". Presumably, the constant influx of bromide ions in our experiment prevented the reservoir concentration from reaching this critical level. The state of the chemistry in the reservoir (excitable or oscillatory) was monitored with a bromide-selective microelectrode [23] whose voltage was amplified and recorded on a strip chart.

To keep the CO_2 that is produced in the BZ reaction from forming bubbles in the reservoir and obscuring the capillaries, the pressure in the reactor was kept above 2 atm by using piston pumps (Pharmacia P-500) and a back pressure valve in the effluent line. If the total flow was 30 ml/h or greater, no bubbles were evident in the reservoir at atmospheric pressure, but under these conditions (in the range of concentrations tested herein) spirals were found to exhibit only simple rotation, possibly due to the formation of microscopic bubbles within the gel. The sulfuric acid/potassium bromide pump required acrylic-coated piston heads because the stock titanium-alloy piston heads were found to dissolve slowly in the sulfuric acid solution and alter the spiral shape and dynamics.

2.2. Reactor operation

The capillary array (Galileo Electro-Optics C25S10M10) is a crucial element of the CFUR. It acts both as a feed to the gel that allows only perpendicular mass transport and as a hydrodynamic flow buffer. If a noncapillary flow buffer such as fritted glass were used in place of the capillary array, mass transport parallel to the gel would occur *within the buffer* and patterns would form there, eliminating the spatial uniformity of the feed to the gel. The capillaries are 10 μm in diameter and 1 mm long, giving each an aspect ratio of 100; this is sufficient to damp out the convection from the stirring of the reservoir, which would distort the patterns in the gel. The capillaries are packed in a hexagonal array, with an open air ratio (porosity) of 0.50 ± 0.02. Thus, a typical wave of 1 mm width is discretely fed by rows of roughly 50 capillaries.

The purpose of the gel is to prevent net mass transport in the system layer above the capillary array; such transport would arise from the radial pressure gradient due to rotary stirring. The gel was prepared according to the recipe in ref. [24].

The lack of any obvious three-dimensional effects (for the concentration range listed above) in a 1 mm thick gel indicated that it was sufficiently thin for the study of two-dimensional wave propagation.

The filter membrane (Whatman cellulose nitrate, 0.2 μm pore size, 130 μm thick) served to provide a white viewing background for the transparent gel, contrasting sharply with the red layer of reagent in which the waves propagate. The blue waves have a small coefficient of extinction and hence appear nearly transparent; they act as narrow, curved windows through which the white background is clearly visible. Since the capillary array is translucent, the background for the waves (without the membrane) would be the red reagent in the reservoir, clearly a poor choice if distinct waves are desired.

The reagent in the reservoir was stirred with a 6 mm diameter cross-shaped magnet at 540 rpm. Exhaustive testing showed that the speed (in the range 150–600 rpm) and direction of rotation of the stirring had no effect on the spirals.

Three to five hours after starting the flow of reactants into the reactor, the reagent in the gel began to oscillate with a period of roughly 10 min, with a slightly higher frequency in the center than elsewhere, leading to target-like phase waves and eventually trigger waves. Additionally, pacemaker sources of target patterns formed near the gel edge where the mixing was less efficient. After several more hours, only trigger waves were observed, produced by a few dominant pacemakers at the edge of the gel. Spiral waves were then initiated by breaking one or more of the trigger waves with light, as described below.

2.3. *Reactor illumination and spiral manipulation*

The large scale properties of the patterns that formed in the gel (cf. plate Ia) were easily observed using fluorescent ring lamps or other similar low intensity light sources. However, in order to follow the tip motion, the width of field was reduced to roughly 6 mm, and more intense illumination was needed. Light from a 100 W mercury arc lamp (Ushio USH-102D lamp, Oriel 66057 housing) was condensed into a uniform, divergent beam that was projected onto the reactor with a beamsplitter, 5°–10° from normal incidence. The light was first passed through a blue-green bandpass filter (λ_{peak} = 512 nm, fwhm = 155 nm) to enhance the contrast and to remove ultraviolet and infrared radiation, which influence wave propagation. The intensity of the light was varied by adjusting the amount of beam divergence with a focusing lens.

Illuminating the gel with the full spectrum produced by the mercury arc lamp (by removing the filter) at an intensity of about 40 mW/cm^2 for 1–2 min acted to reduce the oxidized fronts; thus, selectively exposing small areas resulted in broken waves. Illuminating half of a single trigger wave, from its midst to the perimeter of the gel, resulted in a single free wave end and hence a single spiral. (If more than one spiral were present, a slight spatial gradient in the feed would cause the spirals to rotate at different rates, and eventually the faster spiral would "unwind" the slower and complicate its dynamics appreciably [25].) The asymptotic spiral behavior was attained 5–10 h after initiation.

The presence of a uniform medium near the spiral center is crucial to isolate the true tip dynamics; hence, spirals that formed near the perimeter of the gel were deemed unsuitable for experimental measurements, since the feed is nonuniform at the edge. To produce a more central spiral, either of two methods was used. The first technique was simply to break another wave closer to the center and kill the peripheral spiral with light as described above. The second method was to push the peripheral spiral toward the gel center by imposing a strong light gradient on the spiral, as follows. When the spiral rotation was simple, the size of the circle traced by the tip was found to vary directly with the illumination intensity, and so a spiral would drift perpendicular to any illumination gradient. Fig. 3 illustrates

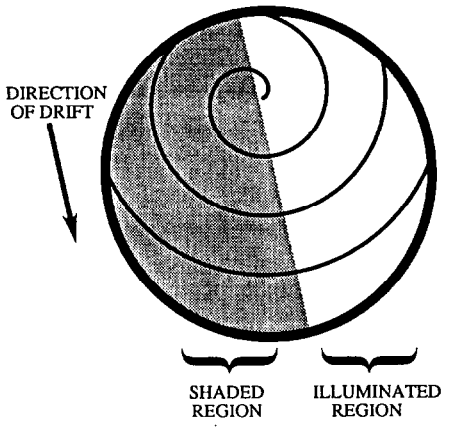

Fig. 3. Schematic of a spiral that is being moved with a strong light gradient, imposed by increasing the incident intensity to 6 mW/cm^2 and blocking the light to part of the medium.

our application of this phenomenon. The semicircles that are traced by the tip in the illuminated region are larger than those in the shaded region, so the spiral moves along the shadow edge in the direction shown. Once the spiral center is at the desired location (requiring several hours), normal illumination is resumed and the chemistry is adjusted to the desired state. The above technique is reminiscent of a procedure used by Agladze et al. [26]; they translated spiral waves by periodically modulating the intensity of a spatially uniform light source.

The intensity of the incident light for general tip tracking purposes was 1.2 mW/cm^2; this intensity was maintained within 5% for each run. No change in the *asymptotic* behavior was observed for intensities ranging from 1 to 3 mW/cm^2. However, a sudden increase of 1 mW/cm^2 was found to perturb the orbital dynamics for several hours, appearing as though the potassium bromate concentration were temporarily decreased by a few percent.

The reactor was illuminated at a slightly oblique angle to avoid intercepting specular window reflections with the camera optics, which were aligned normal to the reactor to interpret the patterns as two-dimensional. Such reflections can be eliminated by using a pair of linear polarizers aligned so as to transmit only the scattered light from the waves. However, a more powerful light source would be required to compensate for the attenuation due to the polarizers.

2.4. *Image processing and data acquisition*

To establish the dynamics of the spiral tip, a small region (25 mm^2) enclosing the tip was monitored using a monochrome video camera (Dage-MTI NC-70, with a Panasonic Newvicon tube) after being magnified with an 80 mm macro lens and autobellows assembly. The tip image from the camera appeared as in plate Ib. The analog video signal was then digitally processed by a frame grabber (Data Translation DT2851) and an auxiliary frame processor (DT2858) installed in an IBM-AT clone. Both processors have 512 lines of resolution, so with a typical width of field of 6 mm, the spatial resolution was about 12 μm per pixel. The dynamic range of intensity for magnified spiral tips was at best about 40 gray levels, out of a possible 256 allowed by the processor boards. This was clearly not taking advantage of the intensity resolution possible, but spatial variations in the illumination ceased to be negligible if the light source was made more intense (spatial gradients of lighting induce spiral drift – see section 2.3). To improve tip definition, we used customized look-up tables with the input video signal domain divided into bands of intensity, typically 4 or 8 gray levels wide. Each of these bands is mapped by the image processor to a specific color; e.g., the first tip of the sequence plate Ic is that from plate Ib after processing. In this way a contour of some specified intensity, designated by the boundary between two colors, can be monitored. In plate Id, for example, one can *define* the tip of the spiral as the point of sharpest curvature on the contour designated by the red/black edge. As long as the illumination intensity could be kept constant, such a definition was maintained from image to image and from

run to run. In the event of a long term intensity fluctuation (between runs), a new contour was selected that enclosed a region of nearly the same width as the old contour with the original intensity.

A full set of intensity bands (as in plates Id and If) was used initially to find an intensity contour that was well defined for the full duration of the run; tracking the contour between the black and the violet in plate Ie, for instance, would have been a poor choice. We chose the contour that enclosed the narrowest region that was well defined for all locations on the orbit. In this way, little ambiguity existed as to where the curvature was maximum along the contour. Lower intensity contours that enclosed wider tips inevitably had flat spots on the end, making tip definition imprecise. In a large majority of the images, the ambiguity was less than 4 horizontal pixel widths, or 45 μm. For all of the spirals observed, the overall size of the orbit was never smaller than 1.1 mm, making this source of error less than 4%.

If a given run were analyzed twice using two different contours, there would be a small difference between the effective locations of the tip in each image, and hence the two orbits would be slightly different, but the qualitative shape of the orbits traced would be the same. One of the observables used to describe the tip orbit (radius ratio – see section 3.1) is dependent on the contour chosen, so to follow this observable with better than 5% accuracy would require a more stable light source than the mercury arc lamp employed here.

Another source of error in establishing the true orbit of the tip arose from the method of illumination. Incident light that was not normal to the plane of the gel distorted the apparent shape and intensity of the spiral tip (due to a shadowing effect) in a way that depends on the orientation of the tip relative to the illumination vector; this produced an apparent elongation of the orbit. The effect is reduced as the amount of obliqueness is decreased, but even at the minimum angle of projection that avoided intercepting specular reflections (about 5°), there was still a small amount of distortion.

Data acquisition was begun once a spiral state was deemed asymptotic. Composite video images were acquired every 30 s (averaged from 5 to 10 images 0.2 s apart to reduce noise; averaging more than 10 frames produced no noticeable improvement) and stored on a 70 Mb hard disk. For the concentrations studied, no additional details of the motion appeared with faster sample rates. Each image requires 256 Kb of memory, so an upper limit on continuous data acquisition was about 2 h.

The steps taken to identify the tip motion in a given run were as follows. First, a computer program recalled an image and performed any desired processing; usually a reference image of a wave-free gel was subtracted from the initial image to remove aberration due to camera optics, and the resulting image was lowpass-filtered (3×3 or 5×5 convolution mask) before mapping to false color in order to remove fuzziness from the contours. Second, a pair of cross hairs was superposed on the image and positioned on the tip by the operator using cursor keys on the AT, and with a carriage return, the pixel location of the tip was entered into memory and the next image in the sequence was recalled. Finally, after processing the entire sequence, the orbit traced by the tip was revealed by converting the successive pixel coordinate pairs into physical coordinates and connecting the points with straight lines.

3. Experimental results

3.1. Comparison to an epicycle

We will describe compound spiral tip orbits by heuristic comparisons with retrograde epicycles, generated by superposing two opposite circular motions having independent radii (r_1, r_2) and rotational frequencies (f_1, f_2), as in fig. 4. In Cartesian coordinates, they are represented para-

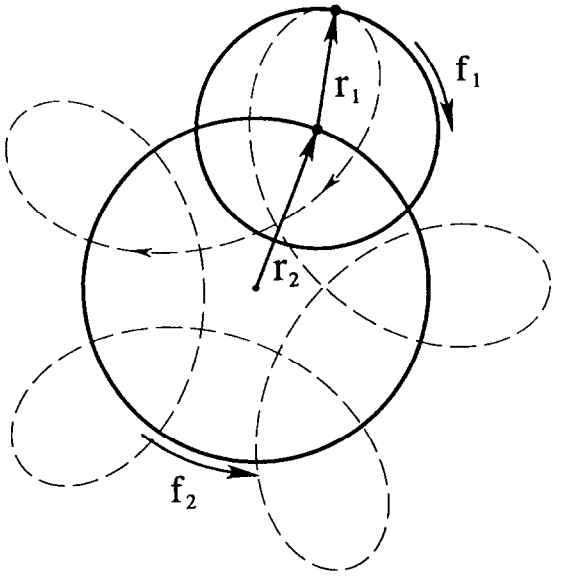

Fig. 4. A retrograde epicycle. The primary circle (radius r_1) orbits the secondary circle (radius r_2) in one direction with frequency f_2, and spins about its center in the opposite direction with frequency f_1; the epicycle is traced by a point fixed on the primary circle. The choice of the primary circle orbiting the secondary circle is arbitrary, for interchanging the two motions alters nothing. Here $r_2/r_1 = 1.43$, $f_1/f_2 = 4$.

metrically by

$$x(t) = r_1 \cos(2\pi f_1 t + \alpha) + r_2 \cos(2\pi f_2 t + \beta). \tag{1a}$$

$$y(t) = r_1 \sin(2\pi f_1 t + \alpha) + r_2 \sin(2\pi f_2 t + \beta). \tag{1b}$$

The primary motion corresponds to the orbit of a spiral tip exhibiting simple rotation with frequency f_1 and radius r_1. The onset of compound rotation is evidenced by the appearance of a secondary motion with frequency f_2 and radius r_2. The retrograde epicycle is defined to within an overall scale factor by the ratio of radii r_2/r_1 and the ratio of rotational frequencies f_1/f_2. Fig. 5 shows a fit of an epicycle to a spiral tip orbit; the values of r_2/r_1 and f_1/f_2 were chosen by hand. Note that if f_1/f_2 is the ratio of two integers p/q, the orbit will close after p primary orbits (or q secondary orbits), and it will have $p + q$ "lobes", or regions of maximum curvature (see also refs. [9, 17, 18]).

3.2. Transition from simple to compound rotation

The data presented here were compiled from runs with twelve distinct batches of chemical solutions, using six gels (two runs per gel). The last four runs were carefully monitored to determine the form of the transition from simple to compound rotation as the potassium bromate concentration was increased.

Fig. 6 shows the asymptotic tip orbits for three different concentrations. Orbits (a) and (b) straddle the transition, which occurred at $[KBrO_3] = 0.0276$ M; orbit (c) is typical of concentrations above transition in the range studied. At the critical concentration, the orbit changed from circles to epicycles and back to circles within several hours, possibly due to fluctuations in pumping speed, light intensity, temperature, etc. Decreasing or increasing the concentration by 1% from

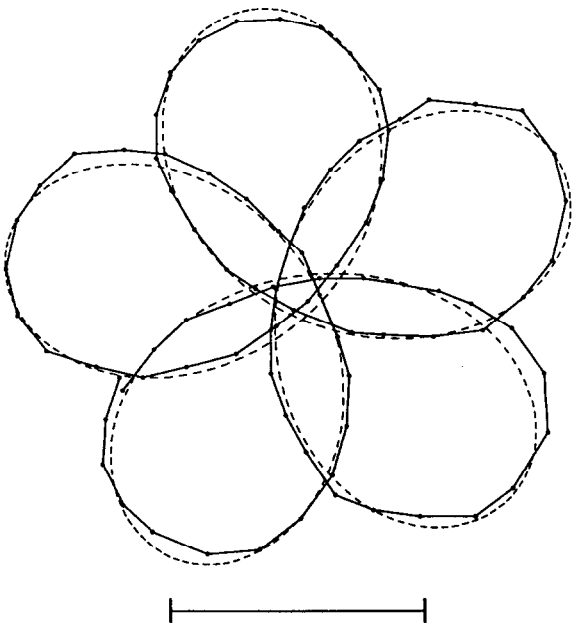

Fig. 5. An epicycle (shown dashed) with $r_2/r_1 = 0.87$ and $f_1/f_2 = 4$ is superposed on a single tip orbit measured at $[KBrO_3] = 0.0323$ M by the method described in section 2.4. The bar represents 1 mm.

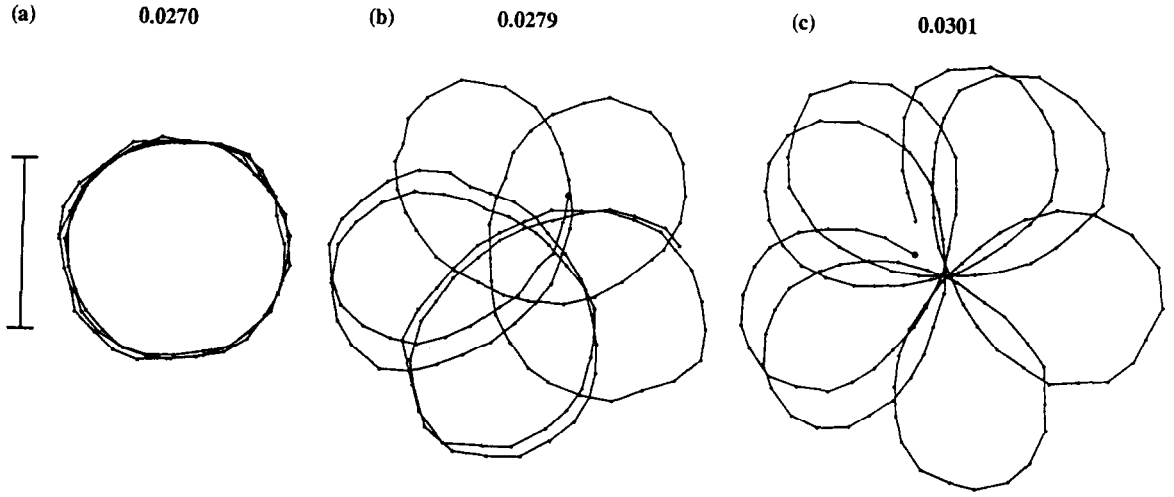

Fig. 6. Spiral tip orbits, obtained at the potassium bromate concentrations shown. The transition from simple to compound rotation occurred at $[KBrO_3] = 0.0276$ M. Orbit (a) represents 45 min, and (b) and (c) each represent 75 min; the sample interval between points was 30 s. The large dots on orbits (b) and (c) were the first points of each tracing. The bar represents 1 mm.

this critical value resulted in the states (a) or (b), respectively. These states were *independent of the path taken in concentration space*, i.e., the transition is apparently *supercritical*. The increase in relaxation time that occurs as a supercritical transition is approached was quite evident. Potassium bromate concentrations differing by 5% or more from 0.0276 M gave spirals that would decay to their asymptotic orbits within 5 h of the last concentration change, but concentrations nearer to the critical value required substantially longer periods of time to settle. For example, orbits at 0.0273 and 0.0279 M required over 24 h to reach their asymptote. (An orbital state was deemed asymptotic if the orbits revealed in repeated tip tracings were the same to within experimental

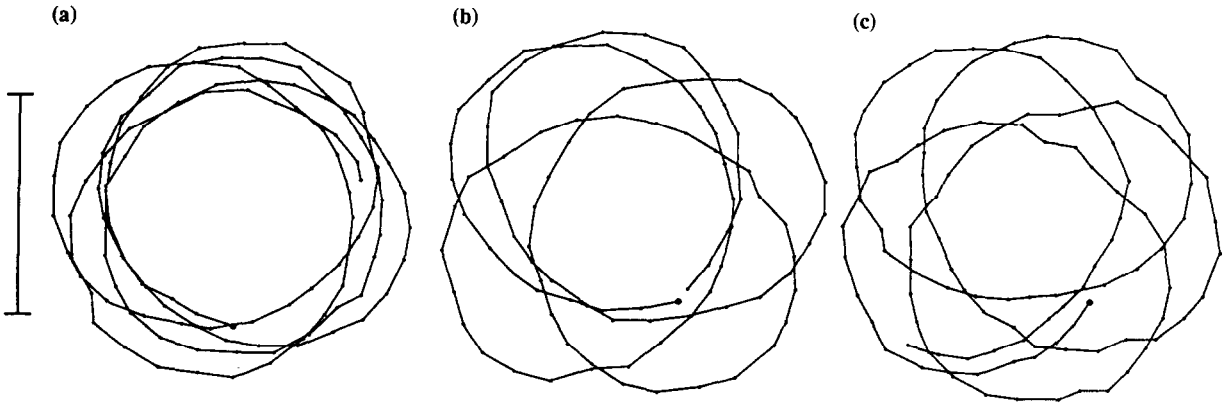

Fig. 7. Transient orbits at the critical concentration, $[KBrO_3] = 0.0276$ M. Transient states can last for several hours before changing, sometimes very gradually and sometimes quite rapidly, to a different state. Other transient states observed at this concentration include circles and epicycles similar to (a) and (b) of fig. 6. The bar represents 1 mm.

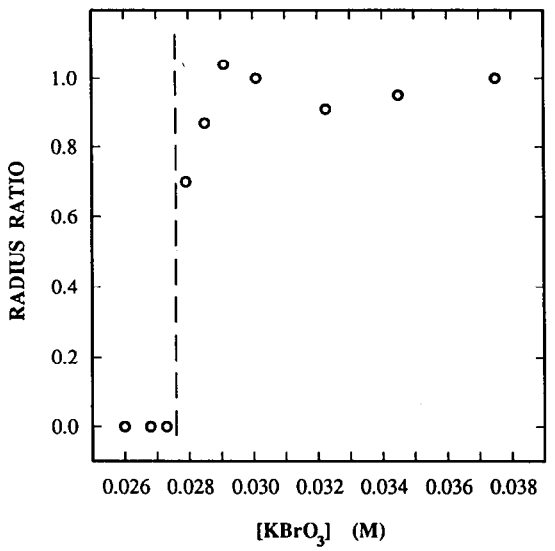

Fig. 8. The ratio r_2/r_1 as a function of the reservoir concentration of potassium bromate. The measurements were obtained by comparing several orbits at each concentration with epicycles.

resolution.) Three transient orbital states typical of those observed at the critical concentration value are illustrated in fig. 7. These states were also briefly observed in the order shown when the concentration was increased to 0.0279 M or higher after stabilizing at 0.0273 M or lower.

The radius ratio, determined by comparison to epicycles, is plotted in fig. 8 as a function of the potassium bromate concentration. Errors as large as 5% may be present due to long-term variations in the light intensity, which change the effective tip location in the video image (section 2.4).

3.3. *Time series construction*

The average reflected light intensity from a fixed square that was small relative to the wave width was monitored in time to better elucidate the dynamics of the tip motion. For simple rotation, the intensity in the square is periodic in time, having a Fourier power spectrum (composed of a fundamental and its associated harmonics) that is independent of the spatial location of the square relative to the spiral center. A time series and its power spectrum are shown in figs. 9a and 9b.

For compound rotation, the intensity in a square very *far* from the center of the spiral is also periodic in time due to the interaction of successive wave fronts. A subtly different time series results when the square is *near the center* (but is never encircled by the tip, i.e., every rotation of the spiral is seen by the square). A portion of a time series, taken 2 mm from the epicycle center of a spiral undergoing compound rotation with $f_1/f_2 \cong 4$ and its power spectrum are shown in figs. 9c and 9d.

The time series for compound rotation is a *frequency-modulated* version of the time series corresponding to simple rotation – the interval between successive passing fronts is not a constant but varies periodically. For compound rotation with a frequency ratio of 4, for example, the frequency of the modulation would be one fourth the frequency of the unmodulated pulses. Compound rotation can be thought of as a cyclic shift of the center about which simple rotation occurs; hence, if the center is moving away from the square, the spiral must rotate through an angle greater than 2π before the wave crosses the square, so the period between the (local) oscillations increases. Conversely, as the center moves toward the square, the period decreases. This effect is discernable in the time series of fig. 9c; there is a periodic fluctuation in the interval between oscillations of about 5% of the average spiral period.

The existence of frequency modulation is readily apparent in the power spectrum of the time series. A generic narrow-band fm signal has sidebands (whose amplitude and shape are functions of the spectrum of the modulating signal) that symmetrically straddle the fundamental and harmonics of the "carrier signal", which for our time series corresponds to the pulse train of local oscillations. These sidebands are quite evident in the power spectrum corresponding to compound rotation (fig. 9d). The modulation frequency can be extracted from the spectrum by determining

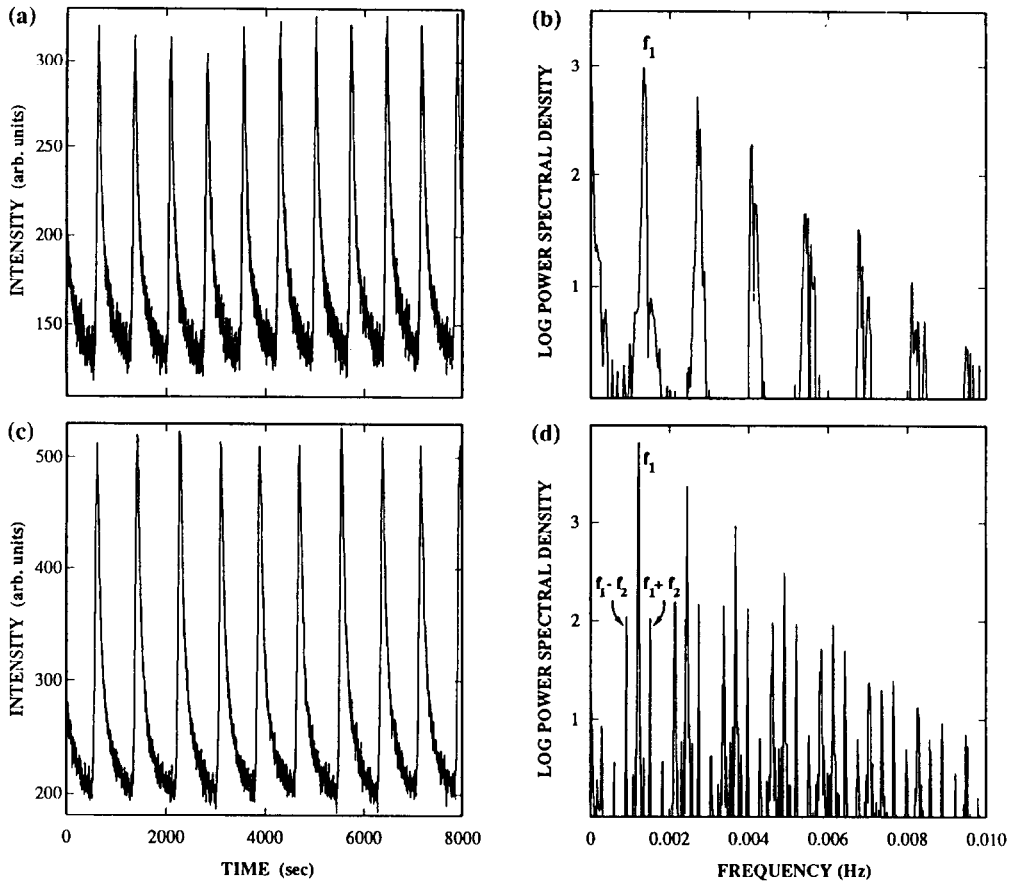

Fig. 9. (a) Average intensity as a function of time inside a 3-pixel (35 μm) square located 3 mm from the center of a spiral undergoing simple rotation ($[KBrO_3] = 0.0270$ M; sample interval, 2 s; duration of entire run, 43200 s). The intensity value for a given sample was determined by averaging 3 video frames, 0.2 s apart, then averaging spatially over the 9 adjacent pixels in the region selected. (b) Power spectrum of the full time series described in (a); f_1 is the frequency of rotation of the tip. (c) Average intensity as a function of time for a spiral undergoing compound rotation ($[KBrO_3] = 0.0281$ M) with $f_1/f_2 \cong 4$ and $r_2/r_1 \cong 1$; the observation square was positioned 2 mm from the center of the epicycle. (The intensity was determined using a camera which has a much better signal-to-noise ratio than the camera used in (a); all other parameters were as in (a).) (d) Power spectrum of the full time series described in (c). The carrier (f_1) and sideband ($f_1 \pm f_2$) frequencies of the compound rotation are identified.

the relative separation of each sideband from its associated carrier harmonic; the ratio of this separation to the separation between the carrier harmonics is the frequency ratio.

We have used the above technique to determine f_1, f_2, and f_1/f_2 as a function of $[KBrO_3]$, as shown in fig. 10. Each data point represents a full 12 h run, just as in fig. 9; they were not collected in any particular order, since earlier runs showed no path dependence. The nearness of the frequency ratio to the integer 4 at the transition (fig. 10c) suggests the possibility of frequency locking [27]. However, frequency locking would result in intervals of control parameter within which the frequency ratio would remain constant, and no such intervals were observed within the resolution of our experiments. Beyond the immediate neighborhood of the transition, clear trends are evident as $[KBrO_3]$ is increased: a linear rise in f_1, a monotonic increase (slower than linear) of f_2, and a monotonic decrease of f_1/f_2.

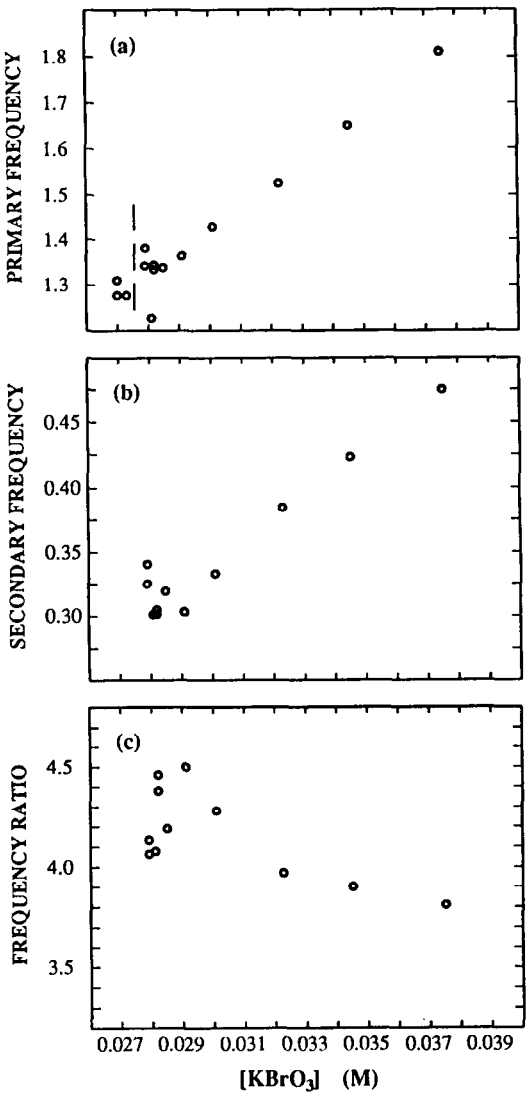

Fig. 10. The primary (f_1) and secondary (f_2) frequencies of spiral rotation (in mHz) and their ratio (f_1/f_2) are plotted in (a)–(c), respectively, as a function of potassium bromate concentration in the reservoir. The dashed line in (a) separates the regions of simple and compound rotation.

3.4. Oscillations in curvature and brightness during compound rotation

A periodic fluctuation in the wave structure was observed near the tip during compound rotation. Note in plate Ie the marked temporal variation in the wave curvature and brightness, indicated by the changing width of the tip enclosed in black. The brightness (blueness in true color) is related to the concentration of ferriin relative to ferroin, and the curvature to which we refer is that of the contour of maximum brightness (not that of a contour surrounding the tip). Plates Id and If illustrate clearly the varying curvature and brightness during different stages of compound rotation. We describe in the following paragraphs the observed sequence of events as a tip traces out a single lobe of its orbit. Refer to fig. 11a for our convention regarding tip motion, and fig. 11b for an illustration of the sequence.

We begin with tip 1 in fig. 11b. Here, the tip appears uniformly bright and propagation is mostly in the normal direction (fig. 11a). Within a few minutes, the tangential component of tip motion grows to nearly the same magnitude as the normal component (tip 3). The result of this motion is a wave with lower curvature and brightness near its tip than elsewhere. The combination of the tangential and normal motions causes the *orbit* traced by the tip to curve sharply. The brightness of the tip region attains a minimum at this stage, which is near the outermost point of the epicycle lobe. Additionally, the width of the *refractory tail* of the wave (represented in plates Id and If by wide green and blue bands behind the front) *gradually* becomes narrower as one moves along the wave toward its tip, and the tip points (i.e. the direction of tangential propagation) into a region that is apparently quiescent. The lack of a substantial refractory tail near the tip presumably allows the portion of the wave nearest its tip to become sharply curved (tip 5 and plate If).

Next, the tip begins to behave *as though a barrier has been erected*, acting to stop tangential motion by reflecting the diffusive flux and causing the tip to grow in brightness. At this stage, the innermost turn of the spiral has three distinct regions (plate If): the tip (brightest), a region of sharp curvature near the tip (dimmest), and the remainder of the wave. The width of the refractory tail now decreases quite sharply near the tip, and the spiral tip points into a region that is

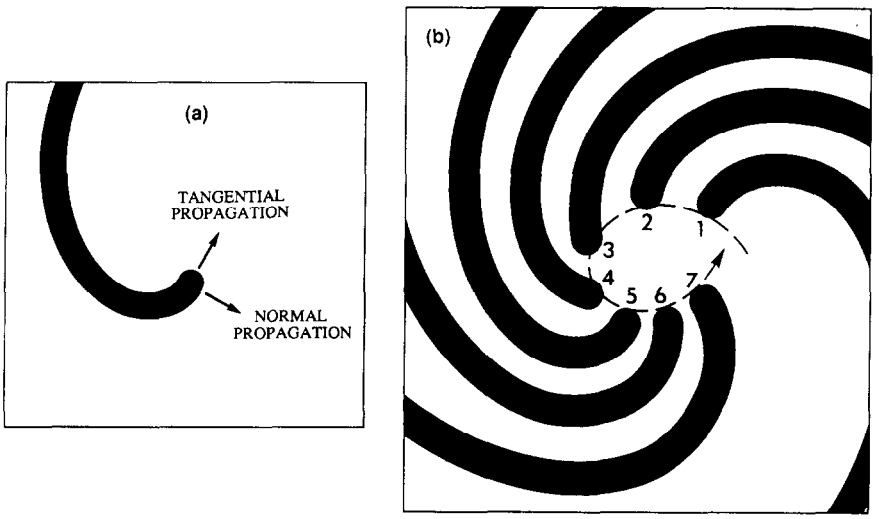

Fig. 11. (a) Schematic showing the components of tip propagation of a counter-clockwise-rotating spiral wave. (b) Qualitative illustration of the spiral tip's changing curvature and the angle of incidence to its path as it traces out a single lobe of a compound orbit. The brightness of the tip (not depicted) steadily decreases in time (tips 1–3) as the front loses curvature and normal incidence, then rapidly increases (tips 4–6) as the front regains curvature and normal incidence.

somewhat refractory, judging by its close proximity to the blue (in our image) tail of the wave that precedes it.

As the tip propagates normal to the "barrier", the wave regains uniform brightness along its length and slowly loses curvature (tip 7), returning to its initial state but offset by some angle (72° if $f_1/f_2 = 4$).

4. Discussion and conclusions

We have examined the transition from simple to compound rotation in repeated runs with increasing and decreasing bromate concentration, and no hysteresis has been observed within the experimental resolution, which suggests that the transition from simple to compound rotation is a supercritical bifurcation. This conclusion is supported by the observed *critical slowing down* – the striking increase in the relaxation time near the transition. Since the transition is apparently continuous and f_2 approaches a nonzero constant as the transition is approached, we conclude that it is likely that the transition is a Hopf bifurcation, even though with our resolution in control parameter r_2/r_1 increases abruptly rather than continuously as would be expected for a supercritical Hopf bifurcation.

Studies of models [5, 9, 15–19, 28–39] have given much insight into the dynamics of chemical spirals, and several models have exhibited a transition from simple to compound rotation [9, 15, 17–19, 32, 38]. Recently the nature of this transition has been examined in detail in studies of two-species models by Barkley et al. [18] and Karma [19]; these simulations clearly showed the transition to be a supercritical Hopf bifurcation. Thus both experiments and simulations indicate that, at least for some parameter values, the transition from simple to compound rotation is continuous.

We searched for frequency locking in the regime with compound rotation in our experiments, and Barkley et al. [18] searched for frequency locking in their numerical simulations; both studies indicate that frequency locking is absent. Perhaps frequency locking is prohibited by some fundamental symmetry, as is the case for traveling waves in a circular system [39].

Our observations lead us to suggest a mechanism for the tip instability that we hope can serve as a guide to future analyses of the spiral tip. We propose that the barrier referred to in section 3.4 is actually the refractory tail of the wave *preceding* the tip, based on the following observations. We observe that as $[KBrO_3]$ is increased, the width of refractory tail (defined by an arbitrary intensity contour) of any wave decreases (see also ref. [20]). Also, in the range of simple rotation, the radius of the orbit (the tip's "turning radius") decreases with increasing $[KBrO_3]$. If the *ratio* of the turning radius to the width of the refractory tail initially decreases as $[KBrO_3]$ is increased, at some point an instability will arise. The tip will try to trace out a small circle, but will only complete a portion of it before further tight turning is impeded by its own refractory wake, making simple rotation impossible, so that compound rotation develops.

For higher $[KBrO_3]$, the ratio of the turning radius to the refractory tail width may increase; if the turning radius were to become sufficiently large in relation to the tail width, the instability would disappear and simple rotation would return. We have observed such a *reverse* transition from compound to simple rotation at $[KBrO_3] = 0.09$ M, but unfortunately the transition was accompanied by oscillations in the reactor reservoir, even with [KBr] as high as 0.01 M (see section 2.1).

In the work of Jahnke et al. [9], the excitability of the medium was decreased (by decreasing $[H_2SO_4]$) and a transition from simple to compound rotation resulted. In our experiments, the excitability was increased (by increasing $[KBrO_3]$) to produce a transition from simple to compound rotation. Hence, it seems likely that there exists a *range of excitability* over which compound rotation is evident. This could be confirmed by further work on the reverse transition noted above.

It is important to note that all of our results were obtained from observations of the recovery species (ferriin), not of the propagator species (bromous acid). Our references to the tip "propagating" are rigorously incorrect, for we can only observe the *result* of the propagation. Until an experimental technique can be found that monitors the propagator wave, we must be content with the results of numerical simulations in revealing its shape and motion.

Our work raises many questions that should be addressed in future studies. Is the functional form of the tip trajectory actually an epicycle? Fig. 5 suggests that there may be a small departure from epicyclic motion (given by eq. (1)); also, Barkley et al. [18] found in their simulations that the paths corresponding to compound rotations were not epicycles. What are the conditions leading to a supercritical or subcritical transition from simple to compound rotation? Does compound rotation always occur over a finite range of control parameter, and if so, does the instability in the tip motion arise from the mechanism suggested above? Our determination of tip orbit parameters presumed a superposition of uniform, circular motions, i.e., the reported values are time averages. What is the time dependence of the tip velocity? Future experiments and numerical and theoretical analyses could provide answers to these questions.

Acknowledgements

We thank A. Arneodo, K. Lee, W.D. McCormick, Z. Noszticzius, W.Y. Tam, and A.T. Winfree for helpful discussions. This work was supported by the Department of Energy Office of Basic Energy Sciences and the Texas Advanced Research Program.

References

[1] A.T. Winfree, When Time Breaks Down (Princeton Univ. Press, Princeton, NJ, 1987) ch. 7, p. 169.
[2] M.A. Allessie, F.I.M. Bonke and F.J.G. Schopman, Circ. Res. 33 (1973) 54; 41 (1977) 9; Clin. Res. 96 (1976) 768.
[3] P.C. Newell and F.M. Ross, J. Gen. Microbiol. 128 (1982) 2715.

[4] S.C. Müller, T. Plesser and B. Hess, Physica D 24 (1987) 87.
[5] J.P. Keener and J.J. Tyson, Physica D 21 (1986) 307; J.P. Keener, SIAM J. Appl. Math. 46 (1986) 1039.
[6] A.T. Winfree, Science 175 (1972) 634.
[7] K.I. Agladze, Proc. Biological Center of Academy of Science, Pushchino, USSR (1983).
[8] K.I. Agladze, A.V. Panfilov and A.N. Rudenko, Physica D 29 (1988) 409.
[9] W. Jahnke, W.E. Skaggs and A.T. Winfree, J. Phys. Chem. 93 (1989) 740.
[10] T. Plesser, S.C. Müller and B. Hess, J. Phys. Chem. 94 (1990) 7501.
[11] F.B. Gulko and A.A. Petrov, Biofizika 17 (1972) 261.
[12] O. Rössler and C. Kahlert, Z. Naturforsch. 34 (1979) 565.
[13] F.J. van Capelle and D. Durrer, Circ. Res. 47 (1980) 454.
[14] A.M. Pertsov, E.A. Ermakova and A.V. Panfilov, Physica D 14 (1984) 117.
[15] V.S. Zykov, Simulation of Wave Processes in Excitable Media (English translation) (Manchester Univ. Press, Manchester, 1987).
[16] J.J. Tyson and J.P. Keener, Physica D 32 (1988) 327; J.J. Tyson, K.A. Alexander, V.S. Manoranjan and J.D. Murray, Physica D 34 (1989) 193.
[17] E. Lugosi, Physica D 40 (1989) 331.
[18] D. Barkley, M. Kness and L.S. Tuckerman, Phys. Rev. A 42 (1990) 2489.
[19] A. Karma, Phys. Rev. Lett. 65 (1990) 2824.
[20] W.Y. Tam, W. Horsthemke, Z. Noszticzius and H.L. Swinney, J. Chem. Phys. 88 (1988) 3395.
[21] Z. Noszticzius, W.D. McCormick and H.L. Swinney, J. Phys. Chem. 91 (1987) 5129.
[22] R.J. Field, E. Körös and R.M. Noyes, J. Am. Chem. Soc. 94 (1972) 8649.
[23] Z. Noszticzius, M. Wittman and P. Sterling, 4th Symp. Ion Selective Electrodes (1984).
[24] Z. Noszticzius, W. Horsthemke, W.D. McCormick, H.L. Swinney and W.Y. Tam, Nature 329 (1987) 619.
[25] V.I. Krinsky and K.I. Agladze, Physica D 8 (1983) 50.
[26] K.I. Agladze, V.A. Davydov and A.S. Mikailov, JETP Lett. 45 (1987) 767.
[27] V.I. Arnold, Geometrical Methods in the Theory of Ordinary Differential Equations (Springer, Berlin, 1983), pp. 304–307, fig. 149.
[28] V.I. Krinsky and B.A. Malomed, Physica D 9 (1983) 81; A.S. Mikhailov and V.I. Krinsky, Physica D 9 (1983) 346.
[29] D. Walgraef, G. Dewel and P. Borckmans, J. Chem. Phys. 78 (1983) 3043.
[30] P.C. Fife, J. Stat. Phys. 39 (1985) 687.
[31] A.B. Rovinsky, J. Phys. Chem. 90 (1986) 217.
[32] V.S. Zykov, Biofizika 31 (1986) 862; 32 (1987) 337.
[33] E. Meron and P. Pelcé, Phys. Rev. Lett. 60 (1988) 1880; E. Meron, Phys. Rev. Lett. 63 (1989) 684; C. Elphick, E. Meron and E.A. Spiegel, SIAM J. Appl. Math. 50 (1990) 490.
[34] D.A. Kessler and H. Levine, Physica D 29 (1989) 1; Physica D, to appear.
[35] I.S. Aranson and M.I. Rabinovich, J. Phys. A 23 (1990) 299.
[36] P.B. Monk and H.G. Othmer, Proc. R. Soc. London B 240 (1990) 555
[37] M.N. Chee, R. Kapral and S.G. Whittington, J. Chem. Phys. 92 (1990) 7302, 7315.
[38] D. Barkley, A model for fast computer simulation of waves in excitable media, in: Proceedings of the Conference on Waves and Patterns in Chemical and Biological Media, Pushchino, USSR, 28 May–1 June, 1990, to be published in Physica D; A coupled-map lattice for simulating waves in excitable media, in: Nonlinear Structures in Physical Systems, eds. L. Lam and H.C. Morris (Springer, Berlin, 1990) p. 192.
[39] D.A. Rand, Arch. Rat. Mech. Anal. 79 (1982) 1.